Journal of Magnetics 17(2), 73-77 (2012) http://dx.doi.org/10.4283/JMAG.2012.17.2.073

Micromagnetic Simulations for Spin Transfer Torque in Magnetic Multilayers

Chun-Yeol You*

Department of Physics, Inha University, Incheon 402-751, Korea

(Received 23 January 2012, Received in final form 2 March 2012, Accepted 5 March 2012)

We investigate spin transfer torque (STT) in magnetic multilayer structures using micromagnetic simulations. We implement the STT contribution for magnetic multilayer structures in addition to the Landau-Lifshitz-Gilbert (LLG) micromagnetic simulators. In addition to the Sloncewski STT term, the zero, first, and second order field-like terms are also considered as well as the effects of the Oersted field due to the running current are addressed. We determine the switching current densities of the free layer with the exchange biased synthetic ferrimagnetic reference layers for various cases.

Keywords : spin transfer torque, magnetic random access memory (MRAM), micromagnetic simulation

1. Introductions

In the theoretical study of spin transfer torque (STT), there are three categories. The main concern of the first one is finding the physical origin of the STT in a given system. The goals of the simple free electron models [1, 2], first principle calculations [3], and Keldysh non-equilibrium Green's function methods [4-7] are all to find the physical origin of the STT term in the given system. These studies reveal the existence of the STT term, what kind of material parameters governs the magnitude of the STT and the bias dependence of in-plane and out-of-plane STT. The second category is the study of spin dynamics with simple macro spin models. By analytically or numerically solving the Landau-Lifshitz-Gilbert (LLG) equation with the additional STT terms, the switching current density can be determined for a given system [8, 9], this is helpful to get a rough idea about spin dynamics under STT. However, in order to investigate the details of the spin dynamics, these macro spin models are too simple and micromagnetic approaches, the third one, are essential. By the virtue of the open source micromagnetic simulation code, OOMMF (Object Oriented MicroMagnetic Frame) [10] and the implementation of the STT in nano-wire geometry [11] many researches about the STT in the domain wall motion of nanowires have been reported [12]. However, so far, there is no open source micromagnetic simulator with an STT term for magnetic multilayer structures including exchange biased synthetic ferrimagnetic reference layers. In this study, we implement an add-on extension module for STT in the magnetic multilayer structures. The developed extension module is based on OOMMF so OOMMF users can easily handle the STT effect in nano-pillar geometry with magnetic multilayers, such as typical STT-MRAM (magnetoresistive random access memory) structures [13-16]. First, we will explain the details of the implementation of the STT module, discuss its usage [17] and present the micromagnetic simulation results with various simulation parameters.

*Corresponding author: Tel: +82-32-860-7667
Fax: +82-32-872-7562, e-mail: cyyou@inha.ac.kr

2. Implementation of STT Term in OOMMF

We add the in-plane and out-of-plane STT terms in LLG equations in order to implement the STT module in OOMMF.

$$\frac{d\vec{m}_s}{dt} = -\gamma\,\vec{m}_s \times \vec{H}_{eff} + \alpha\,\vec{m}_s \times \frac{d\vec{m}_s}{dt} - \gamma\, a_J \vec{m}_s \times (\vec{m}_s \times \vec{m}_p) - \gamma\, b_J (\vec{m}_s \times \vec{m}_p) \quad (1)$$

Here, $a_J = a_1 J$, $a_1 = \eta_P \frac{\hbar}{2e\mu_0 M_s d_s}$, $b_J = (b_0 + b_1 J + b_2 J^2)$

and J is current density (opposite to the electron flow), and $\vec{m}_{s,p}$ are unit vectors of the magnetization of switching and polarizer layers, respectively. We consider the zero-th, first, and second order field-like terms in order to handle the most general cases [14-16]. η_p is the spin

polarization of the polarizer layer, or the spin torque efficiency. We set η_p to 0.7 for our study and d_s is the thickness of the switching layer. In the present implementation, a_1 is automatically determined from the given parameters. According to the theoretical work [18], η_p has an angular variation, however, we ignore the angular dependence of η_p in our implementation for simplicity. It must be noted that we assume STT is an interface term, as such, we replace d_s with the unit cell thickness of the z-direction in the above relation. Therefore, the STT term acts only on the first unit cells of the switching layer, and acts on the next unit cells coupled with first unit cells only through atomic exchange coupling. In this way, a thicker switching layer can be handled automatically. We will discuss the switching layer thickness dependence of the switching current density later.

The direction of positive current is defined from the bottom to top of the nano-pillar as shown in the Fig. 1. It must emphasized that positive (negative) current prefers anti-parallel (parallel) states, because electron flows are opposite to the current direction.

The Oersted field generated by a running current in the nano-pillar structure is numerically calculated by separate procedures, and this calculated Oersted field is treated as an external field. The magnitude of the Oersted field is determined by the current density and nano-pillar geometry. It must be mentioned that we assume a uniform current density, even though the real current density is non-uniform during the switching processes due to a relatively large tunneling magneto-resistance (TMR) in MgO based junctions. Using built-in exchange bias and interlayer exchange coupling energy, typical STT-MRAM structures, AFM (anti-ferromagnetic), synthetic ferrimagnet (F_3/NM/F_2), Insulator (I), and free (F_1) layers are successfully modeled and examined in this study. Where, $F_{1,2,3}$ are ferromagnetic layers and NM is non-magnetic layer, respectively. More details of their usages can be found in [17].

3. Results and Discussions

We consider typical STT-MRAM structures, as shown in the Fig. 1. The saturation magnetization M_s and thicknesses of $F_{1,2,3}$ layers are 1.3×10^6 A/m and 2 nm, respectively, except when we investigate the F_1 layer thickness dependence. The thicknesses of the NM and I layers are 1 nm. The cross-section of the nano-pillar is an ellipse of 60×40 nm^2, where the unit cell size is $1 \times 1 \times 1$ nm^3. The exchange bias field of 4×10^5 A/m is assigned to the +x-direction for the F_3 layer. A strong antiferromagnetic interlayer exchange coupling energy -1×10^{-3} J/m^2 is applied between F_2 and F_3 layers in order to keep a strong antiferromagnetic coupling between them. No crystalline anisotropy energy is considered in this study for simplicity. The exchange stiffness constant A is set to 2.0×10^{-11} J/m and the Gilbert damping constants α are varied from 0.005 to 0.05.

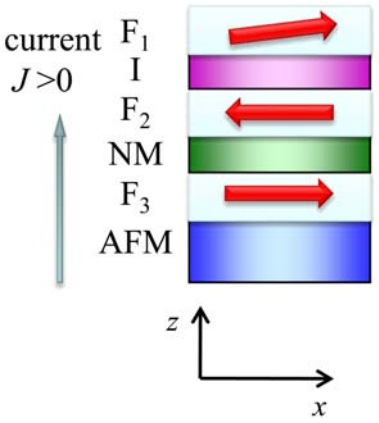

Fig. 1. (Color online) The typical STT-MRAM structure. $F_{1,2,3}$ are the ferromagnetic and NM, I, AFM are the non-magnetic, insulator, antiferromagnetic layers, respectively. The positive current density is defined from the bottom to top, and x-axis is long axis of the ellipse.

Fig. 2 shows the hysteresis loop of the F_1 layer. Due to stray field from the synthetic ferrimagnet (F_3/NM/F_2) structure, the loop is shifted by −17 kA/m from the loop center. The stray field causes different switching current densities from the P (parallel) to AP (anti-parallel)-state and from the AP to P-state. It must be noted that the

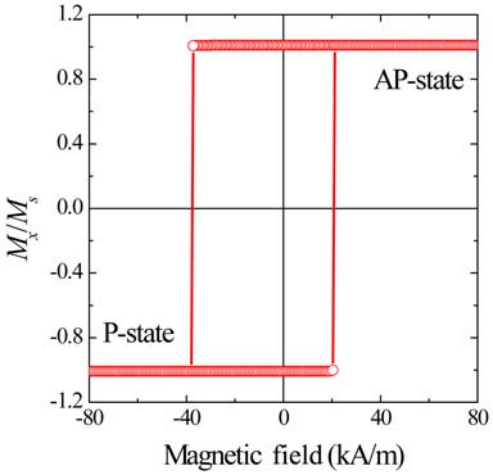

Fig. 2. (Color online) Magnetization hysteresis loop of the F_1 layer. The hysteresis loop is shifted by the stray field from the synthetic ferrimagnet structure (F_3/NM/F_2). Within the swept field range, the magnetization of F_2 and F_3 layers are almost fixed.

micromagnetic simulation reveals that the stray field from the synthetic ferrimagnet in the F_1 layer position varies from −1.2 to −31 kA/m (from center to edge). Therefore, this −17 kA/m shift is reasonable.

The switching current density J_c is

$$J_c \sim \frac{\alpha}{a_1}\left[H_{eff} + \frac{1}{2}(N_y + N_z - 2N_x)M_s\right], \quad (2)$$

for the macro-spin model [8, 9]. Where $N_{x,y,z}$ are the demagnetization factors of the F_1 layer, where $N_z = 1$, $N_x = N_y = 0$ for a thin film and $H_{eff} = H_{ext} + b_J + H_{stray} + H_{Oe}$ is the effective field including an external field term, H_{ext}, a field like term, b_J, a stray field term, H_{stray}, and a Oersted field term, H_{Oe}.

In order to determine the switching current density, we perform a micromagnetic simulation with a given current density of 10 ns, and then wait for 2 ns more without current. After the 12 ns simulation time, we check the magnetization configuration and decide the switching status. Using this procedure, first, we varied the F_1 thickness, d_s, from 1~4 nm and then found J_c for each thickness. The results are depicted in Fig. 3 for P- to AP-state switching. The symbols represent the micromagnetic simulation results and the solid line is a linear fit. As shown in Fig. 3, the dependence of the switching current density on d_s is well fitted with a linear line, this is due to the inverse proportionality of a_1 to d_s. Since we assume the STT acts as only the interface to the first unit cell of the switching layer, this linearity is expected. We find that the linearity breaks down when $d_s \geq 5$ nm in our simulations. With a thicker d_s, the bottom of the F_1 layer is switched where spin torque is exerted, but the upper part of F_1 layer is not switched together due to the finite exchange length. Therefore, a twisted domain wall is formed between the bottom and top layer [1]. Because the exchange length of switching layer is of the order of a few nm, this is a reasonable result. However, if the domain wall is formed in real experiments, additional spin torque is created due to non-collinear alignment of the magnetization inside of the switching layer. This additional spin torque will move the domain wall. However, this kind of spin torque is not implemented in our simulations. Therefore, we have to limit our simulations to a thin switching layer, and the exchange length determines this limited thickness.

Second, we show the Gilbert damping parameter, α, dependence on J_c in Fig. 4. Equation implies the switching current density is proportional to α. A linear dependence is clearly shown in Fig. 4 for P- to AP-state and AP- to P-state. If we calculate the slope of the relation $J_c \sim D\alpha$, $D = 1/a_1(\pm H_{stray} \pm H_{Oe} + (1/2)M_s)$ from the given parameters, we obtain $D_{P\text{-}AP} = 9.0$ and $D_{AP\text{-}P} = 9.5 \times 10^{12}$ A/m^2 without consideration of the Oersted field. The slopes from the micromagnetic simulations give $D_{P\text{-}AP} = 11.9$ and $|D_{AP\text{-}P}| = 12.4 \times 10^{12}$ A/m^2. Even though there are small discrepancies in the absolute magnitudes between the analytic and micromagnetic results, the difference between the P- to AP-state and AP- to P-state switching current densities, $D_{AP\text{-}P}$ - $D_{P\text{-}AP}$, are similar for both cases, this implies the origin of the difference between switching current densities is the stray field [20]. The small discrepancies between the analytic expressions and micromagnetic simulation indicate the limits of the macro-spin model. The macro-spin model ignores spin wave excitation with short wavelengths (see Fig. 5(b) and (c)). Since short

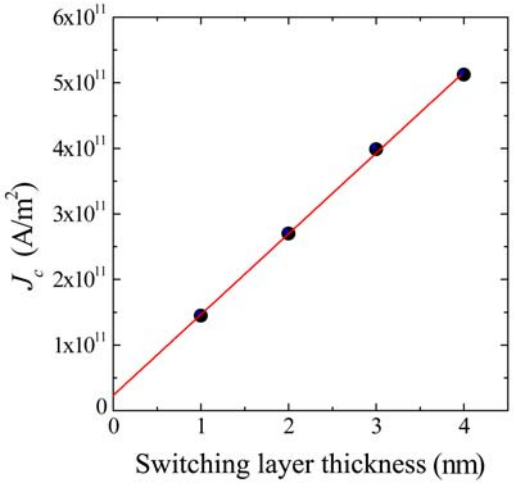

Fig. 3. (Color online) The switching current densities J_c as a function of the switching layer thickness for P- to AP-state switching. The symbols are micromagnetic simulation results and solid line is a linear fit.

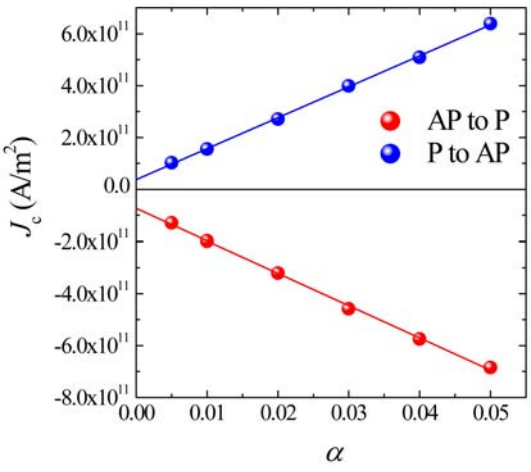

Fig. 4. (Color online) The switching current densities J_c as a function of the Gilbert damping parameter α for P- to AP-state (blue symbols) and AP- to P-state (red symbols). The solid lines are linear fits.

wavelength spin wave excitation is important in the switching procedure, the analytic expression cannot be correct. One more finding from our simulation results is the finite interception when $\alpha \to 0$. According to the analytic model, J_c goes zero with α. However, the micromagnetic simulation reveals J_c has a finite value when $\alpha \to 0$. The physical reason behind this finite interception is not clear at this stage. Even though the values are not large (–7.32 and 3.74×10^{10} A/m^2 for the AP- to P-state and P- to AP-state, respectively), it may be important to reduce the J_c for small α materials.

Fig. 5(a)-(d) show snap shots of the F_1 layer magnetization configurations during the switching processes. With a current density of 2.7×10^{11} A/m^2 and α of 0.02, the magnetization of F_1 layer switches from the P-state to AP-state at t = 9.0 ns as shown in Fig. 5(e). According to Fig. 5(e), the magnetization oscillates after 2 ns, but it takes 6-7 ns for the switching occur. During that period, the magnetization oscillates as shown in Fig. 5(a). The spins oscillate and the directions of the spin are opposite at the edges. A C-type domain structure is formed, this implies the macro-spin model cannot describe the state seen Fig. 5(a). At t = 7.7 ns, the spin dynamics get more complex, as shown in Fig. 5(b). The domain structure is S-type and the instability of the domain structure increases with the spin polarized current. At t = 8.8 ns, shown in Fig. 5(c), most spins point toward the short axis of the ellipse and finally complete switching occurs after 9.0 ns, as seen in Fig. 5(d). Different values for α give similar spin dynamics.

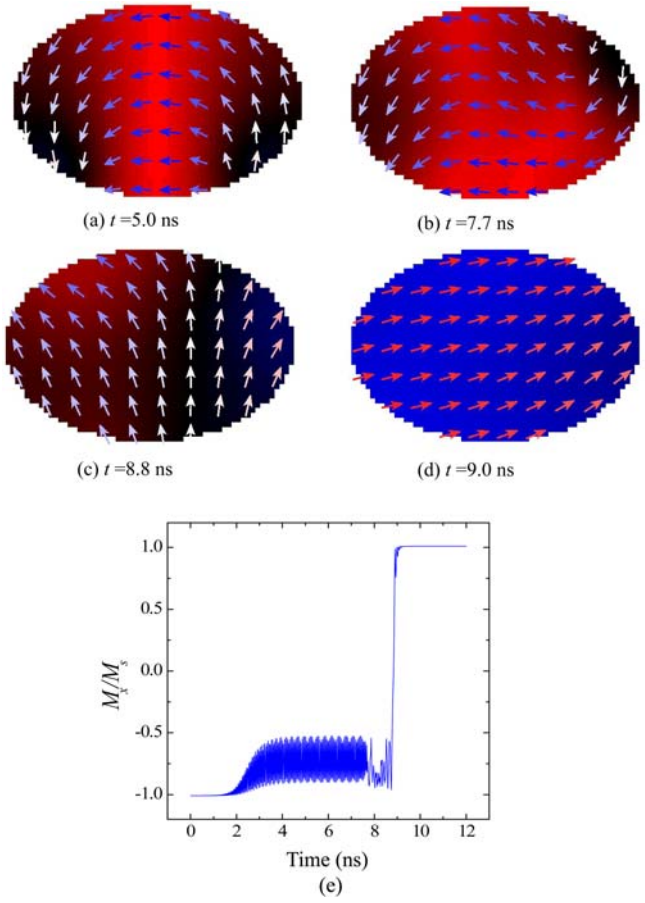

Fig. 5. (Color online) The snap shots of the magnetization configuration of the F_1 layer with $J = 2.7 \times 10^{11}$ A/m^2 at (a) t = 5.0, (b) 7.7, (c) 8.8 and (d) 9.0 ns, respectively. (e) The magnetization dynamics as a function of the time for α = 0.02.

We can include or exclude the numerically pre-calculated Oersted field, which is generated by the current in the simulations. The effect of the Oersted field is not serious in the determination of the switching current density. However, the Oersted field changes the details of the spin dynamics. Figure 6 shows the magnetization switching from AP- to P-state with a current density of -1.84×10^{11} A/m^2 with and without the Oersted field for the α = 0.01 case. As shown in Fig. 6, the switching still occurs without the Oersted field, while the switching does not occur with the Oersted field. However, the difference in switching current density is not noticeable in many cases.

It must be mentioned that we do not show the effect of a field like term in this work. Since the role of the field-like term is somewhat tedious, furthermore the proper field-like term contribution is not clear yet [13-16]. However, it is already implemented in our extension module, so there is no limitation in the study of the field-like term contribution.

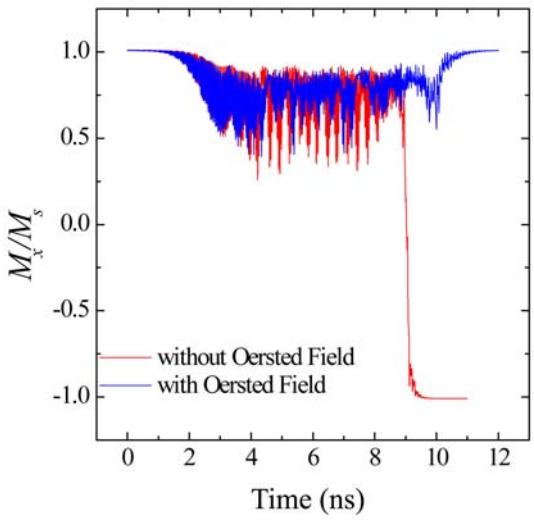

Fig. 6. (Color online) The magnetization dynamics from AP- to P- state as a function of the time for α = 0.01 with and without the Oersted field generated by the spin polarized current of -1.84×10^{11} A/m^2.

4. Conclusions

We implement an STT extension module for OOMMF. With the STT extension module, we simulate the spin dynamics for typical STT-MRAM structures, these consist of an exchange biased synthetic ferrimagnetic layer and a free layer with an insulator layer. We find that the switching current densities for P- to AP-state and AP- to P-state are different even though we set the a_1 to be identical for both cases. The small difference in the switching current densities is ascribed to the stray field from the exchange biased synthetic ferrimagnetic layer.

Acknowledgements

This work was supported by (2010-0022040) programs through a NRF grant funded by MEST.

References

[1] J. C. Slonczewski, J. Magn. Magn. Mater. **159**, L1 (1996).
[2] L. Berger, J. Appl. Phys. **49** (1978) 2156: L. Berger, Phys. Rev. B **54**, 9353 (1996).
[3] C. Heiliger and M. D. Stiles, Phys. Rev. Lett. **100**, 186805 (2008).
[4] C.-Y. You, J.-H. Han, and H.-W. Lee, Thin Solid Films **519**, 8247 (2011).
[5] I. Theodonis, N. Kioussis, A. Kalitsov, M. Chshiev, and W. H. Butler, Phys. Rev. Lett. **97**, 237205 (2006).
[6] D. M. Edwards, F. Federici, J. Mathon, and A. Umerski, Phys. Rev. B **71**, 054407 (2005).
[7] C.-Y. You, S.-H. Song, and H. Kim, Appl. Phys. Lett. **519**, 8247 (2011).
[8] C.-Y. You, J. Appl. Phys. **107**, 073911 (2010).
[9] C.-Y. You, Curr. Appl. Phys. **10**, 952 (2010).
[10] http://math.nist.gov/oommf.
[11] http://www.zurich.ibm.com/st/magnetism/spintevolve.html.
[12] J. B. Yoon, C.-Y. You, Y. H. Jo, and S.-Y. Park, and M.-H. Jung, Appl. Phys. Exp. **4**, 063006 (2011).
[13] H. Kubota, A. Fukushima, K. Yakushiji, T. Nagahama, S. Yuasa, K. Ando, H. Maehara, Y. Nagamine, K. Tsunekawa, D. D. Kjayaprawira, N. Watanabe, and Y. Suzuki, Nature Phys. **4**, 37 (2008).
[14] J. C. Sankey, Y.-T. Cui, J. Z. Sun, J. C. Slonczewski, R. A. Buhrman, and D. C. Ralph, Nature Phys. **4**, 67 (2008).
[15] S.-C. Oh, S.-Y. Park, A. Manchon, M. Chshiev, J.-H. Han, H.-W. Lee, J.-E. Lee, K.-T. Nam, Y. Jo, Y.-C. Kong, B. Dieny, and K.-J. Lee, Nature Phys. **5**, 898 (2009).
[16] M.-H. Jung, S. Park, C.-Y. You, and S. Yuasa, Phys. Rev. B **81**, 134419 (2010).
[17] For more details, http://spintronics.inha.ac.kr/STT-OOMMF.html
[18] J. C. Slonczewski, Phys. Rev. B **71**, 024411 (2005): J. C. Slonczewski and J. Z. Sun, J. Magn. Magn. Mater. **310**, 169 (2007).
[19] W. J. Kim, T. D. Lee, and K.-J. Lee, Appl. Phys. Lett. **93**, 232506 (2008).
[20] In this study, we assumed the a_1 is the same for P- to AP-state and AP- to P-state switching for the simplicity. Therefore, the different switching current density is due to the extrinsic reason such as stray field.